



저작자표시-비영리-변경금지 2.0 대한민국

이용자는 아래의 조건을 따르는 경우에 한하여 자유롭게

- 이 저작물을 복제, 배포, 전송, 전시, 공연 및 방송할 수 있습니다.

다음과 같은 조건을 따라야 합니다:



저작자표시. 귀하는 원저작자를 표시하여야 합니다.



비영리. 귀하는 이 저작물을 영리 목적으로 이용할 수 없습니다.



변경금지. 귀하는 이 저작물을 개작, 변형 또는 가공할 수 없습니다.

- 귀하는, 이 저작물의 재이용이나 배포의 경우, 이 저작물에 적용된 이용허락조건을 명확하게 나타내어야 합니다.
- 저작권자로부터 별도의 허가를 받으면 이러한 조건들은 적용되지 않습니다.

저작권법에 따른 이용자의 권리는 위의 내용에 의하여 영향을 받지 않습니다.

이것은 [이용허락규약\(Legal Code\)](#)을 이해하기 쉽게 요약한 것입니다.

[Disclaimer](#)

藥學碩士 學位論文

Crystal structure of human endothelial
overexpressed lipopolysaccharide-associated
factor 1

Human endothelial overexpressed
lipopolysaccharide-associated factor 1의 결정화
및 구조 규명

2017年 8月

서울대학교 大學院
藥學科 醫藥生命科學專攻
Minju Kim

Abstract

Endothelial-overexpressed LPS-associated factor 1 (EOLA1) is a novel gene discovered in an effort to identify genes expressed in endothelial cells by activation of lipopolysaccharide. Previous study demonstrates that knocking down EOLA1 stimulated interleukin-6 (IL6) and apoptosis in the treatment of LPS in human umbilical vein endothelial cells (HUVEC). Analysis of the sequence of EOLA1, revealed that it has ASCH (activating signal cointegrator-1 homology) domain containing a unique β -barrel fold similar to pseudouridine synthase and archaeosine transglycosylase (PUA) domain. Because PUA domain is an ancient RNA binding domain, both ASCH and PUA domain appear to have arisen from a common RNA binding precursor. Here, I report the crystal structure of EOLA1 at 1.7 Å resolution by single wavelength anomalous dispersion (SAD) method using selenomethionine derivative crystals to solve the phasing problem. I demonstrated that EOLA1 could bind with RNA through gel mobility shift assay. Based on these results, I propose that EOLA1 is a RNA binding domain and would play regulatory roles in transcription or in protection of HUVEC injury with inflammation.

Keywords: endothelial-overexpressed LPS associated factor 1, RNA binding domain, PUA domain, crystal structure, protein X-ray crystallography

2014-22967

Contents

Abstract	i
Contents	iii
List of Figures	v
List of Tables	vi
I. Introduction	1
II. Materials and Methods	4
1. Materials	4
2. Methods	4
2.1. Cloning	4
2.2. Overexpression	5
2.3. Purification	5
2.4. Crystallization	6
2.5. X-ray data collection and structure determination	6
2.6. Electrophoretic mobility shift assay (EMSA)	7
III. Results and Discussion	
1. Cloning	8
2. Overexpression and purification	8
3. Crystallization	16
4. X-ray data collection and structure determination	17
5. Electrophoretic mobility shift assay (EMSA)	19
6. Overall structure of EOLA1	21
7. Structure analysis	22

IV. References	27
V. Acknowledgement	30
Abstract in korean	31

List of Figures

Figure 1.	SDS-Page of expression and solubility test of full-length EOLA1 at 293 K	9
Figure 2.	Purification profile from the HiTrap chelating HP column chromatography	10
Figure 3.	SDS-PAGE analysis of HiTrap chelating HP column fractions	11
Figure 4.	Purification profile from the HiTrap Q HP column chromatography	12
Figure 5.	SDS-PAGE analysis of HiTrap Q HP column fractions	13
Figure 6.	Purification profile from HiLoad 16 600 Superdex 75 pg column chromatography	14
Figure 7.	SDS-PAGE analysis of HiLoad 16 600 Superdex 75 pg fractions	15
Figure 8.	Native EOLA1 protein crystal	16
Figure 9.	SeMet-substituted EOLA1 protein crystal	16
Figure 10.	X-ray diffraction image from native EOLA1 crystal	17
Figure 11.	Electrophoretic mobility shift assay (EMSA) gel result	20
Figure 12.	Overall structure of EOLA1	21
Figure 13.	Sequence analysis of EOLA1 and ASC1	24
Figure 14.	GxK motif of EOLA1	25
Figure 15.	Electrostatic potential surface of EOLA1	26

List of Tables

Table 1.	Data collections statistics for native EOLA1	18
----------	----------------------------------------------	----

I. Introduction

Endothelial-overexpressed lipopolysaccharide associated factor 1 (EOLA1) is a novel gene discovered in an effort to identify genes expressed in endothelial cells by activation of lipopolysaccharide (LPS) [1]. The protein is primarily expressed in heart, skeletal muscle, kidney, liver, placenta and relatively high levels in spleen, colon, small intestine, and cancer cell lines. [2]. Previous report indicates that the protein is localized in the nucleus and matrix of ECV304 (human umbilical vein endothelial cell line) cells, and may play a role as a signal transduction factor [3, 4]. LPS is an endotoxin composed of lipid and polysaccharide that is found in the outer layer of most gram-negative bacteria. It initiates strong immune response in immune systems and presence of LPS could induce septic shock due to severe immune response. The endothelial cell is a prime target of the LPS molecule, and vascular complications of septic shock due to Gram-negative bacteria are associated with endothelial injury [5, 6]. Recent studies indicate that LPS induces apoptosis in different types of endothelium such as HUVEC [7, 8].

The two-yeast hybrid system showed interaction between EOLA1 and metallothionein (MT) -2a, which was demonstrated by co-immunoprecipitation experiment [1]. MTs are cysteine rich, low molecular mass (6-7 kDa) metal binding proteins that are found in many tissues [9]. Main

biological roles of metallothioneins are: 1) maintenance of the intracellular homeostasis of essential transition metals, 2) detoxification of nonessential metals and, 3) a protective function against intracellular oxidative stress [10, 11]. MT2a is present in all organs and further studies revealed that MT2a is induced by LPS which is involved in cell proliferation and differentiation [2, 12]. Previous study shows that EOLA1 could inhibit IL-6 expression and apoptosis in LPS treated HUVEC cells which suggests that EOLA1 could play a regulatory role in stress such as inflammation [2]. Furthermore, knocking down EOLA1 significantly decreased the expression of MT2a which is activated by LPS and inhibiting MT2a increased IL-6 expression of LPS induced HUVEC cells [2]. These findings demonstrate that EOLA1 plays a regulatory role in transcription and protection of HUVEC injury in inflammation [2].

Sequence analysis of EOLA1 revealed an activating coactivator complex-1 homology (ASCH) domain, which contains a unique β -barrel fold similar to pseudouridine synthase and archaeosine transglycosylase (PUA) domain. PUA domain is an RNA binding domain and both ASCH and PUA domains appear to have arisen from a common RNA-binding precursor [13]. However, the differences in their binding cleft resulted in distinct functional roles and thus, ASCH domains are likely to possess RNA-binding site [13]. ASCH

domain was named after ASC-1, which is a novel transcription coactivator molecule of nuclear receptors [14]. Analysis of EOLA1 structure by Dali Server revealed structural similarity in the ASCH domain between ASC-1 and EOLA1 with Z-score of 12.3.

To further study the biological role of EOLA1, I have determined its three-dimensional structure. Full length of EOLA1 was overexpressed with C-terminal His6-tag in *Escherichia coli*, purified, and crystallized. Phasing problem was solved by using selenomethionine (SeMet)-substituted EOLA1. The three-dimensional structure was determined by single wavelength anomalous diffraction (SAD). Here, I report the crystal structure of EOLA1, elucidating the potential function of the protein.

II. MATERIAL AND METHODS

1. Materials

Human full-length EOLA1 (158 amino acids) gene synthesis and polymerase chain reaction (PCR) primers, which were used for EOLA1 gene amplification, were purchased from Bioneer and Cosmogentech (Seoul, Korea), respectively. Luria Broth was purchased from LPHA and Kanamycin from BioBasic. Restriction enzymes (*NcoI* and *XhoI*) and polymerase PrimeSTAR[®] HS DNA Polymerase from Enzynomics and TaKaRa (Korea) respectively. The expression vector pET-28a(+) and *E.coli* Rosetta[™] 2(DE3) pLysS competent cells were obtained from Novagen (Darmstadt, Germany). Crystal screen solution Crystal Screen 1+2 and Index were purchased from HAMPTON Research.

2. Methods

2.1. Cloning

Full construct of EOLA1 (158 amino acid residues), was amplified by PCR using PrimeSTAR[®] HS DNA Polymerase (TaKaRa). Amplified genes were cleaved at *NcoI* and *XhoI* restriction enzyme sites, which were inserted into the *NcoI/XhoI*-digested expression vector pET-28a(+) (Novagen) with C-

terminal His6-tag.

2.2. Overexpression

The recombinant plasmid was transformed into *E.coli* Rosetta™ 2(DE3) pLysS competent cells. Cells were grown at 310 K and 0.5 mM isopropyl 1-thio-β-D-galactopyranoside (IPTG) were added at O.D.600nm of 0.6 in Luria Broth culture media containing 30 mg ml⁻¹ kanamycin. When overexpressing SeMet-substituted EOLA1 in Rosetta™ 2(DE3) pLysS, I used the M9 cell culture medium containing extra amino acids supplemented with SeMet.

2.3. Purification

Cell lysis was carried out using a cell disruptor (Sonics, Vibracell VCX750) in 50 mL of lysis buffer containing 500 mM NaCl, 20 mM Tris-HCL, 35 mM imidazole, pH 7.5 and 1 mM phenylmethylsulfonyl fluoride. The crude lysate was centrifugated at 35,000 xg for 60 min at 277 K. The supernatant was loaded onto HiTrap Chelating HP column (GE Healthcare) for affinity chromatography and eluted with elution buffer (500 mM NaCl, and 1 M imidazole, pH 7.5). Sample was further purified by anion exchange chromatography (HiTrap 5 mL Q HP, GE Healthcare) and size exclusion chromatography (HiLoad 16 600 Superdex 75 pg, GE Healthcare) equilibrated with 200 mM NaCl, 10 mM Tris-HCL, pH 7.5. The purified protein was concentrated to 10 mg/ml⁻¹. Purification of SeMet-substituted protein was the

same as above.

2.4. Crystallization

EOLA1 crystals used for data collection were grown with 1 μl of protein and 0.5 μl of solution (0.1 M HEPES, 4.3 M NaCl, pH 7.5) with protein concentration of 15.65 mg ml^{-1} using hanging drop diffusion method. The Se-Met substituted EOLA1 was also crystallized by using the same reservoir as the native crystal.

2.5. X-ray data collection and structure determination

Prior to data collection, crystals were cryo-protected by soaking them in reservoir solution of 0.1 M HEPES, 4.3 M NaCl, pH 7.5 with 10% glycerol. X-ray diffraction data for both native and SeMet crystals were collected at the synchrotron BL-7A at the Pohang Accelerator Laboratory. The SeMet-substituted EOLA1 crystals were also cryo-protected using selenomethionine derivative crystals to solve the phasing problem. The native crystal structure was solved by single wavelength anomalous dispersion (SAD) method using the *HKL2000* [15] program package. SAD phases were determined by using AUTOSOL of the PHENIX software [16]. Structure of EOLA1 was completed by repeated cycles of model building using *Wincoot* [17] and refinement by *REFMAC* [18]. Refinement steps were monitored using an R_{free} value based

on 5.0% of the independent reflections.

2.6. Electrophoretic mobility shift assay (EMSA)

0.1mM of EOLA1 and 0.1mM of tRNA (Yeast tRNA from brewer's yeast, Roche) were incubated in 1:1 ratio for one hour at 4°C. Also, 0.1mM of Triosephosphate isomerase from *Thermoplasma acidophilum* (TaTPI) was incubated with 0.1mM of tRNA in 1:1 ratio, which was used as a control for this assay.

III. Results and Discussion

1. Cloning

Full length of human EOLA1 was constructed as a recombinant protein with C-terminal His6-tag in pET-28a vector to enable selectivity in purification.

2. Overexpression and Purification

To find the *E. coli* strain most suitable for overexpression of EOLA1, I tested 11 competent cells for overexpression. Test result showed that EOLA1 was most soluble in Rosetta™ 2(DE3) pLysS competent cells. SeMet-substituted EOLA1 was also expressed in Rosetta™ 2(DE3) pLysS using M9 cell culture medium containing amino acids supplemented with SeMet. The IPTG induced cells were harvested by centrifugation at 6,000 g for 10 min at 277 K. The wet cell weight about 5.5 g. Centrifuged cells were lysed by sonication and the recombinant EOLA1 protein was purified by affinity chromatography, anion exchange chromatography, and size exclusion chromatography.

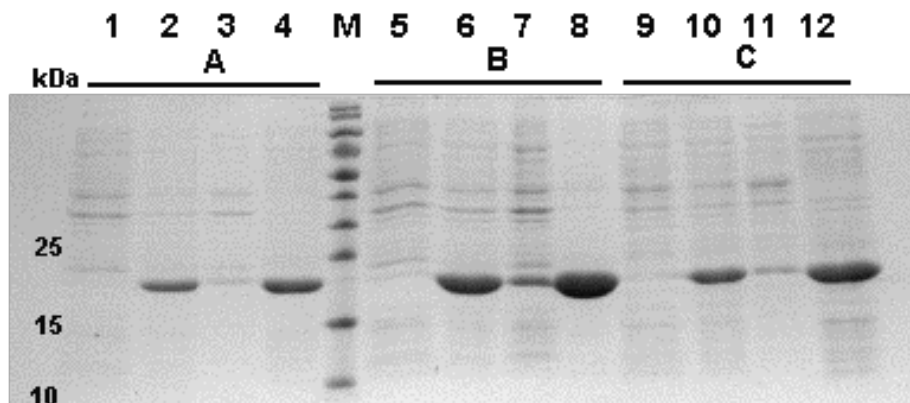


Figure 1. SDS-Page of expression and solubility test of full-length EOLA1 at 293 K.

A) Rosetta™ 2 (DE3)

B) Rosetta™ 2 (DE3) pLysS

C) SoluBL21™

Lane 1: **A**, before IPTG induction

Lane 2: **A**, after IPTG induction

Lane 3: **A**, supernatant fraction

Lane 4: **A**, pellet fraction

Lane M: protein marker

Lane 5: **B**, before IPTG induction

Lane 6: **B**, after IPTG induction

Lane 7: **B**, supernatant fraction

Lane 8: **B**, pellet fraction

Lane 9: **C**, before IPTG induction

Lane 10: **C**, after IPTG induction

Lane 11: **C**, supernatant fraction

Lane 12: **C**, pellet fraction

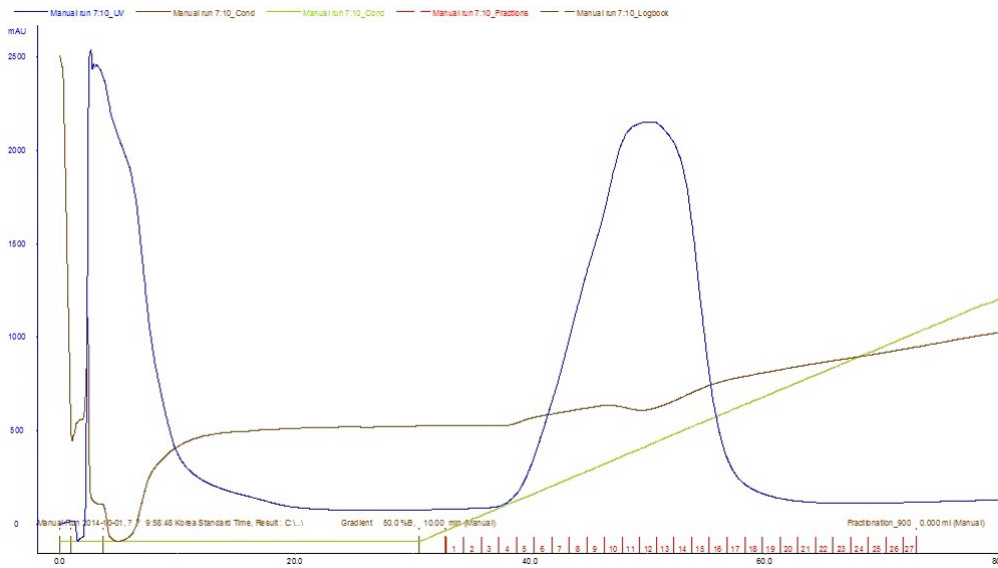


Figure 2. Purification profile from the HiTrap chelating HP column chromatography

Elution was performed with 1 M imidazole in 20 mM Tris-HCl at pH 7.5, and 500 mM NaCl.

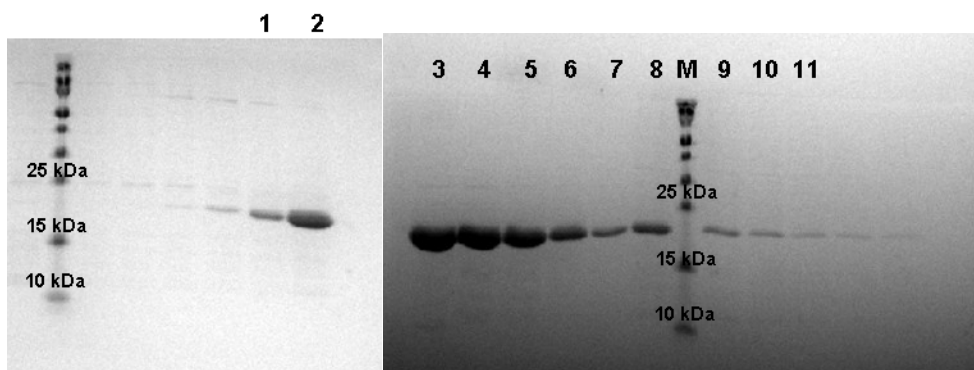


Figure 3. SDS-PAGE analysis of HiTrap chelating HP column fractions

- Lane 1: fraction #5
- Lane 2: fraction #8
- Lane 3: fraction #11
- Lane 4: fraction #13
- Lane 5: fraction #14
- Lane 6: fraction #15
- Lane 7: fraction #16
- Lane 8: fraction #17
- Lane M: protein marker
- Lane 9: fraction #18
- Lane 10: fraction #19
- Lane 11: fraction #20

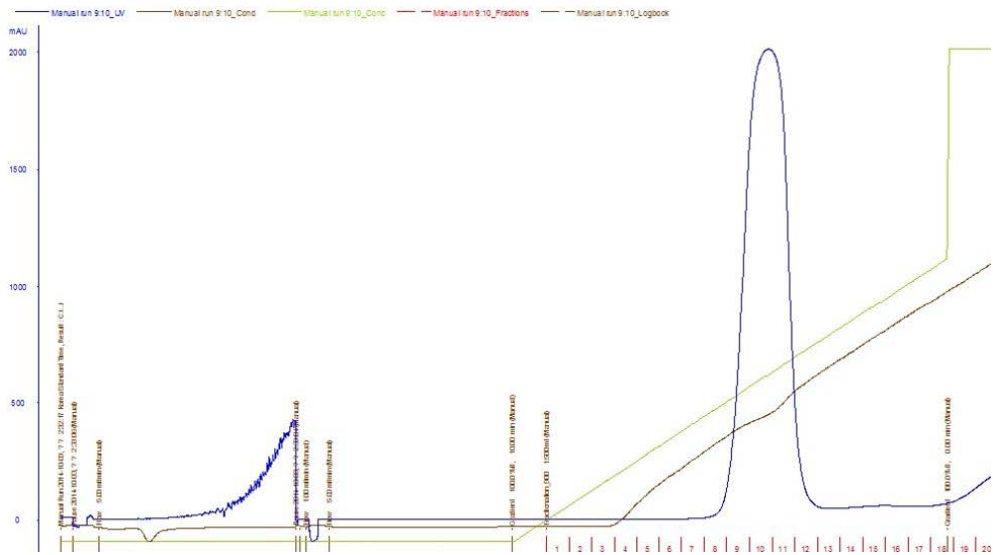


Figure 4. Purification profile from HiTrap Q HP column chromatography

Elution was performed with 1 M HCl in 20 mM Tris-HCl at pH 8.0

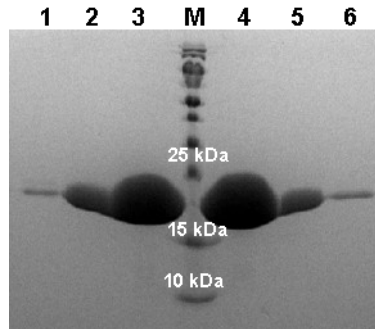


Figure 5. SDS-PAGE analysis of HiTrap Q HP column fractions

Lane 1: fraction #8

Lane 2: fraction #9

Lane 3: fraction #10

Lane M: protein marker

Lane 4: fraction #11

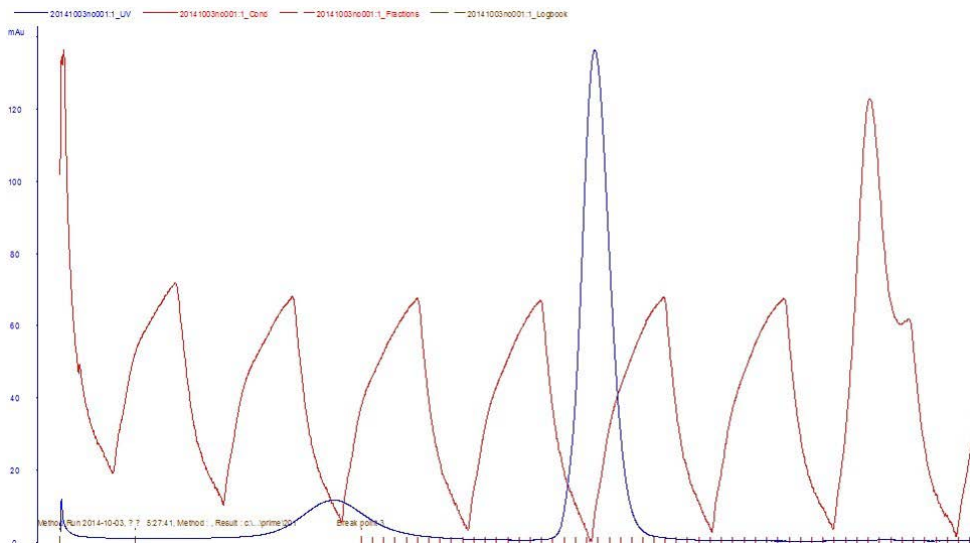


Figure 6. Purification profile from HiLoad 16 600 Superdex 75 pg column chromatography

Gel filtration was performed in 200 mM NaCl in 10 mM Tris-HCl at pH 7.5.

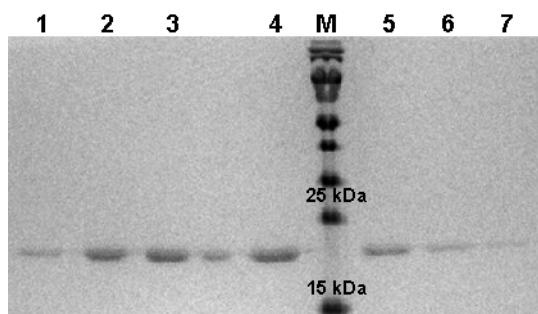


Figure 7. SDS-PAGE analysis of HiLoad 16 600 Superdex 75 pg fractions

Lane 1: fraction #19

Lane 2: fraction #20

Lane 3: fraction #21

Lane 4: fraction #22

Lane M: protein marker

Lane 5: fraction #23

Lane 6: fraction #24

Lane 7: fraction #25

3. Crystallization

After purification, protein was concentrated to 15.65 mg ml^{-1} and crystallized using the hanging drop diffusion method at 295 K using the reservoir of 0.1 M HEPES, 4.3 M NaCl, at pH 7.5. SeMet substituted EOLA1 crystals were obtained by using the same conditions as above.

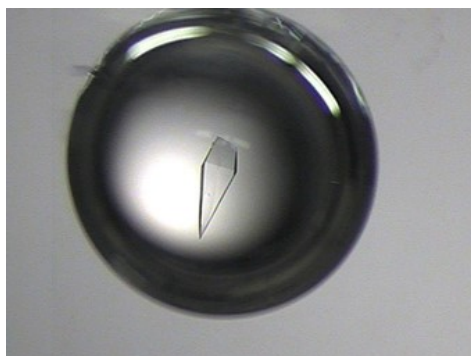


Figure 8. Native EOLA1 protein crystal

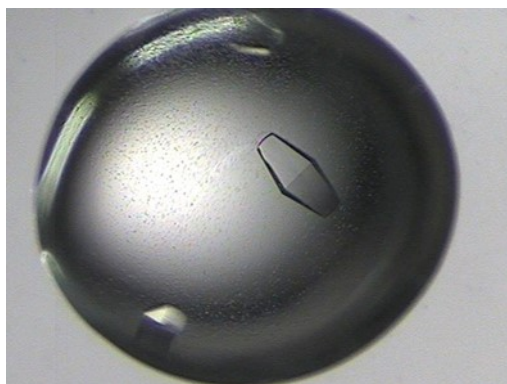


Figure 9. SeMet-substituted EOLA1 protein crystal

4. X-ray data collection and structure determination

X-ray diffraction data for native EOLA1 crystal was collected to 1.71 Å at the synchrotron BL-7A at the Pohang Accelerator Laboratory. Native crystals belong to space group $P4_12_12$ with unit cell parameters of $a = 49.8$ Å, $b = 49.8$ Å, $c = 175.7$ Å, and $\beta = 90^\circ$. Table 1 provides the summary of data collection on native EOLA1 crystal.

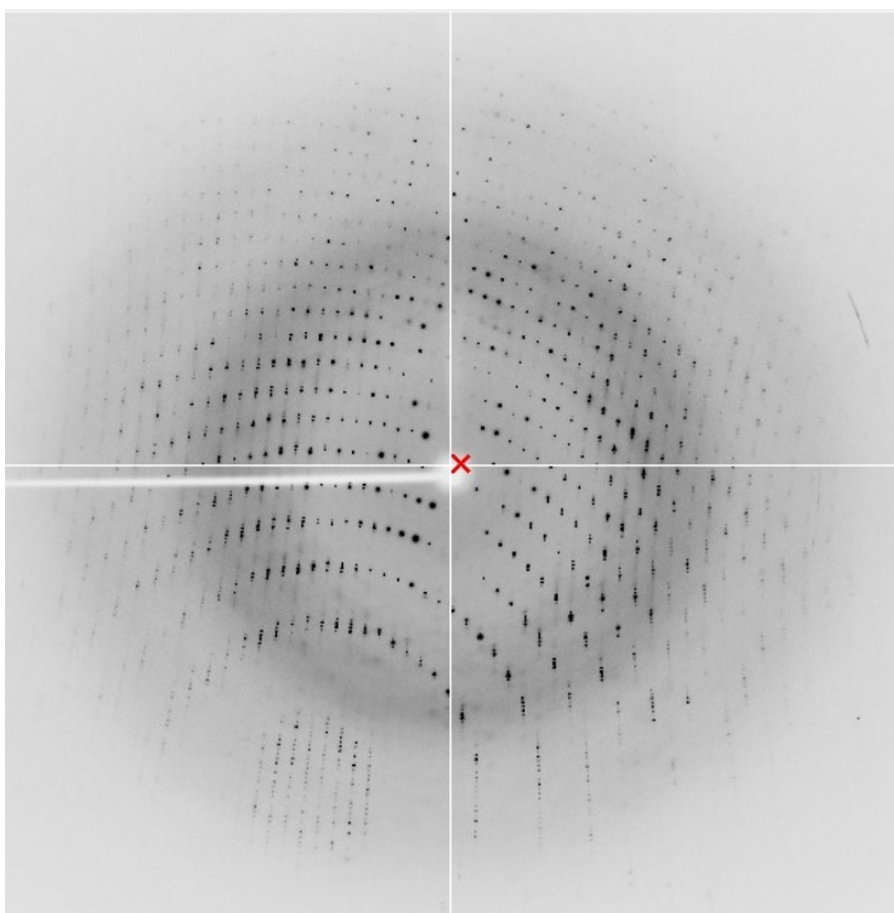


Figure 10. X-ray diffraction image from native EOLA1 crystal

Table1 1. Data collection statistics for native EOLA1

Data collection	Human EOLA1
Space group <i>a</i> , <i>b</i> , <i>c</i> (Å), β (°)	P4 ₁ 2 ₁ 2 49.8, 49.8, 175.7, 90
Data set	
X-ray wavelength (Å)	1.0000
Resolution (Å) ^a	50-1.71 (1.75-1.71)
Total / unique reflections	428,745/24,867
Completeness (%)	99.82
R _{merge} (%) ^b	20.4 (58.3) ^a
Refinement	
Resolution (Å)	50-1.71
R _{work} ^c / R _{free} ^d (%)	21.25 / 25.48
Ramachandran plot analysis (%)	
Most favored regions	95.6
Additional allowed regions	3.1
Outliers	1.3

^aValues in parentheses indicate the highest resolution shell

^b $R_{\text{merge}} = \frac{\sum_h \sum_i |I(h)_i - \langle I(h) \rangle|}{\sum_h \sum_i I(h)_i}$, where $I(h)$ is the intensity of reflection h , and \sum_h is sum of overall reflection, and \sum_i is the sum over i measurement of reflection h .

5. Electrophoretic mobility shift assay (EMSA)

To examine the tRNA binding affinity of EOLA1, EMSA was performed by incubating EOLA1 and 0.1mM of yeast tRNA mixture in 1:1 ratio for one hour at 4°C. For control of this assay, 0.1mM of Triosephosphate isomerase from *Thermoplasma acidophilum* (TaTPI) was incubated with 0.1mM of tRNA in 1:1 ratio. After the incubation, samples were loaded onto agarose gel (1%) and gel electrophoresis was initiated for 15 minutes. The result showed that there is an interaction between EOLA1 and tRNA in comparison to TaTPI and tRNA, which was used as a control in this experiment. The dragged band in EOLA1 and tRNA clearly indicate that the protein interacted with the mixture of tRNA. In contrast, TaTPI and tRNA mixture showed no significance of binding activity showing one clear band of tRNA. However, because tRNA mixture was used for the gel mobility shift assay, it seems like more than one tRNA with different sizes interacted with EOLA1 causing a broad band in the agarose gel. Nonetheless, EMSA confirms that EOLA1 does bind with tRNA and the ASCH domain may act as an RNA binding site.

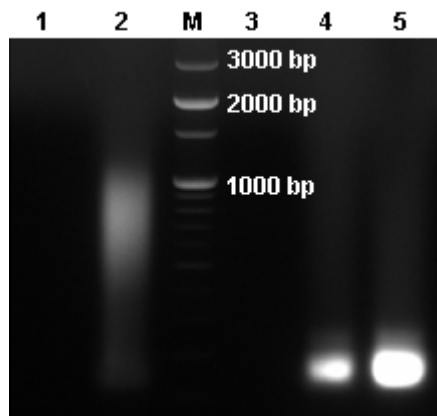


Figure 11. Electrophoretic mobility shift assay (EMSA) gel result

Lane 1: EOLA1

Lane 2: EOLA1 + tRNA mix

Lane M: DNA marker

Lane 3: TaTPI

Lane 4: TaTPI + tRNA

Lane 5: tRNA

6. Overall structure of EOLA1

The structure of human EOLA1 was determined at 1.71 Å resolution by Single wavelength anomalous dispersion (SAD) using selenomethionine derivative crystals to solve the phasing problem. Final model of EOLA1 consist of five α -helices (α A- α E) and six β -sheets (β 1- β 6).

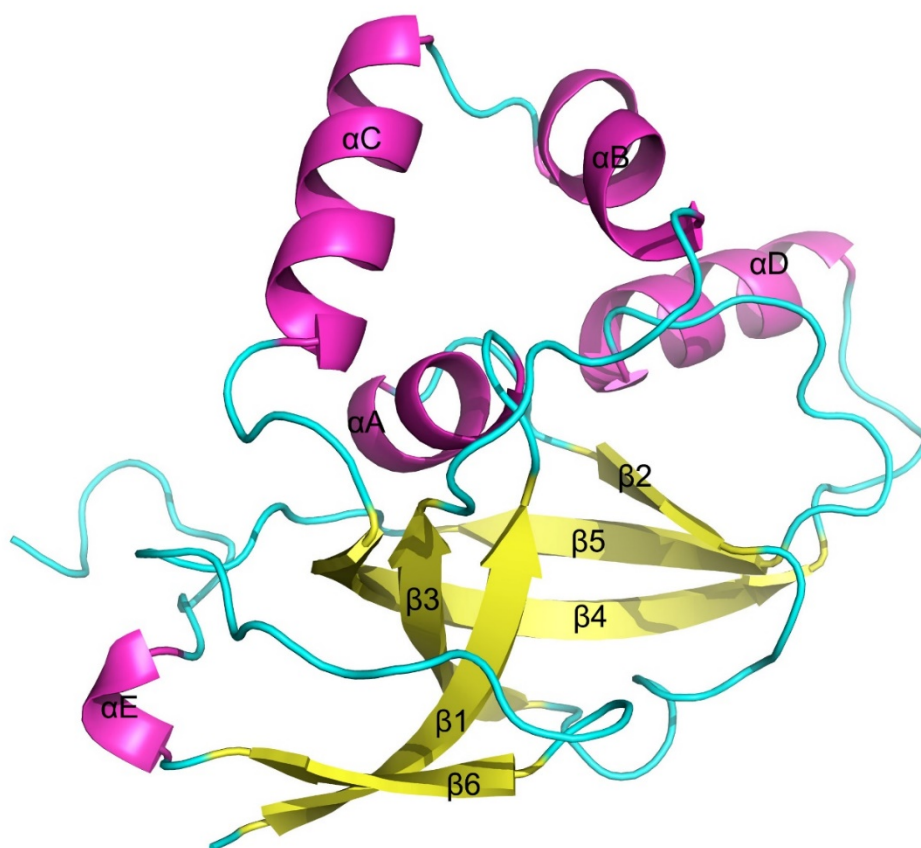


Figure 12. Overall structure of EOLA1

7. Structure analysis

Sequence analysis of EOLA1 revealed an activating signal cointegrator-1 homology (ASCH) domain, which contains a unique β -barrel fold similar to pseudouridine synthase and archaeosine transglycosylase (PUA) domain. ASCH domain was named after ASC-1, which is a novel transcription coactivator molecule of nuclear receptors [14]. PUA domain is an RNA binding domain and both ASCH and PUA domains appear to have arisen from a common RNA-binding precursor [12]. However, the differences in their binding cleft resulted in distinct functional roles and thus, ASCH domains are likely to possess RNA-binding site [12]. In terms of conserved sequences, EOLA1 contains a GxKxxxxR (where x is any amino acid) motif (Gly19-Ile20-Lys21-Thr22-Val23-Glu24-Thr25-Arg26) at the N-terminal domain and a GxK motif (Gly19-Ile20-Lys21) in between the core helix and strand-2, which are all characteristics of ASCH domain [12]. Most of ASCH domains have two conserved residues (E,T,S and R) located next to each other that leads to a longer G-x-K-x-[ETS]-x-R motif [15]. PUA domains use the glycine-containing loop between α A and β 1 for RNA interaction and these surfaces are often composed of positively charged side chains [11]. Since ASCH conserved domain, GxKxxxxR motif is also located in the loop between α A and β 1, these observations indicate that ASCH will also contact the RNA molecule using the

glycine-containing loop. Therefore, I suggest that EOLA1 will also use its loop located in the GxKxxxxR motif to interact with RNA molecule.

EOLA1, like all proteins containing ASCH domain, contains a helix between strand 1 and strand 2 and two helical segments between strand-4 and strand-5 with six β -strands that form a β -barrel. However, unlike most ASCH domain containing proteins which contain five β -strands, EOLA1 contains six β -strands, which differs from most ASCH domains. Despite this difference, the β -barrel folds of EOLA1 is still very similar when compared to other proteins containing ASCH domain. ASCH superfamily contains a distinct cleft located between the helix and β -strand 2. The GxK motif is located in this cleft and forms a positively charged surface [12]. Similar cleft has also been observed in the PUA domain which has been predicted to be involved in RNA methylase and likely to function as RNA binding surface [16-18]. The GxK motif in EOLA1 containing lysine is located between αA and $\beta 1$ forming a cleft with positively charged surrounding surface. This cleft exists in both ASCH and PUA domain and is predicted to function as RNA binding surface. Thus, I suggest that the same cleft in EOLA1 will also possess RNA-binding activity.

A

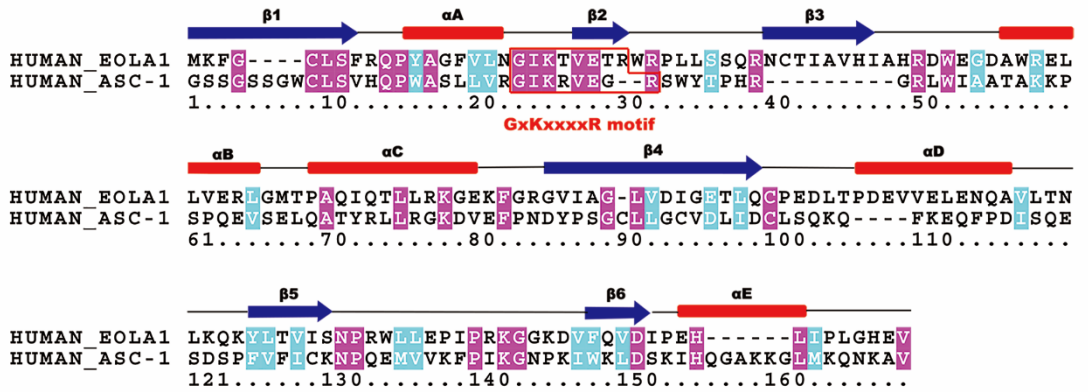


Figure 13. Sequence analysis of EOLA1 and ASC1

(A) Sequence alignment of ASC-1 and EOLA1. GxKxxxxR motif is highlighted in red.

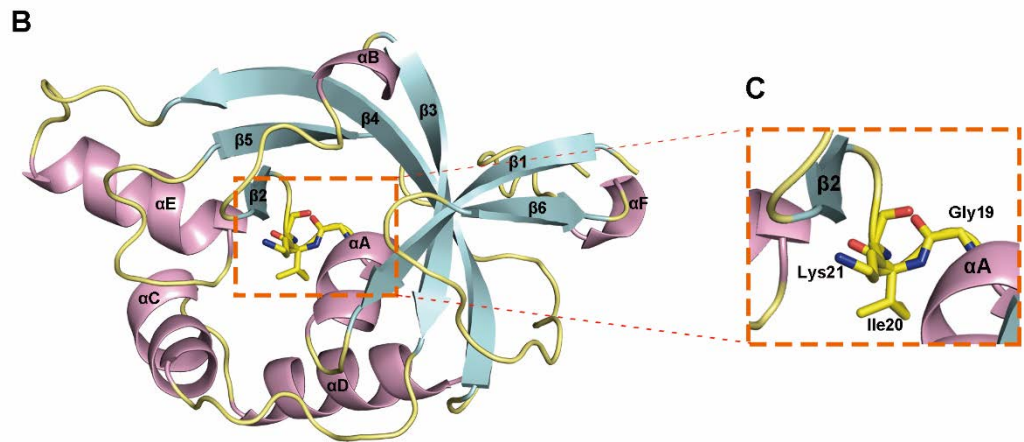


Figure 14. GxK motif of EOLA1

(B) Overall structure of EOLA1. Five alpha helices (αA - αE , purple) are shown in purple and six β -sheets ($\beta 1$ - $\beta 6$, blue) are shown in yellow. The six β -sheets form a unique β -barrel shape similar to ASCH domain. (C). GxK motif (Gly19-Ile20-Lys21) in between the core helix αA and strand-2.

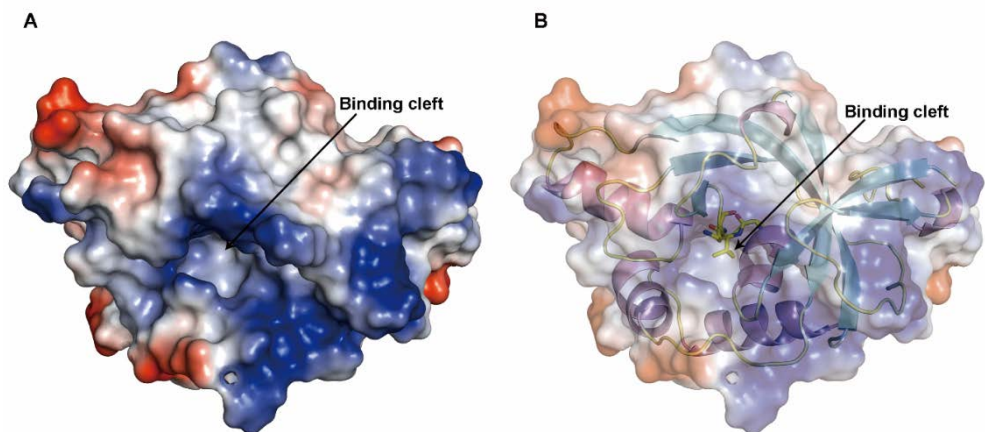


Figure 15. Electrostatic potential surface of EOLA1.

(A) Overall surface of electrostatic potential with binding cleft labeled. (B)

Secondary structure of EOLA1 is shown in cartoon with transparent electrostatic potential surface map.

IV. Reference

1. Liang, Z. and Z. Yang, *Identification and characterization of a novel gene EOLA1 stimulating ECV304 cell proliferation*. Biochem Biophys Res Commun, 2004. **325**(3): p. 798-802.
2. Liu, Y., et al., *EOLA1 protects lipopolysaccharide induced IL-6 production and apoptosis by regulation of MT2A in human umbilical vein endothelial cells*. Mol Cell Biochem, 2014. **395**(1-2): p. 45-51.
3. Kato, Y., et al., *Augmentation of lipopolysaccharide-induced thymocyte apoptosis by interferon-gamma*. Cell Immunol, 1997. **177**(2): p. 103-8.
4. Cai, Z., et al., [*Purification of human endothelial overexpressed lipopolysaccharide-associated factor 1 protein*]. Zhonghua Shao Shang Za Zhi, 2005. **21**(5): p. 367-9.
5. Cybulsky, M.I., M.K. Chan, and H.Z. Movat, *Acute inflammation and microthrombosis induced by endotoxin, interleukin-1, and tumor necrosis factor and their implication in gram-negative infection*. Lab Invest, 1988. **58**(4): p. 365-78.
6. Pober, J.S. and R.S. Cotran, *The role of endothelial cells in inflammation*. Transplantation, 1990. **50**(4): p. 537-44.

7. Koide, N., et al., *Apoptotic cell death of vascular endothelial cells and renal tubular cells in the generalized Shwartzman reaction*. FEMS Immunol Med Microbiol, 1996. **16**(3-4): p. 205-11.
8. Messmer, U.K., V.A. Briner, and J. Pfeilschifter, *Tumor necrosis factor-alpha and lipopolysaccharide induce apoptotic cell death in bovine glomerular endothelial cells*. Kidney Int, 1999. **55**(6): p. 2322-37.
9. Inoue, K., et al., *Metallothionein as an anti-inflammatory mediator*. Mediators Inflamm, 2009. **2009**: p. 101659.
10. Thornalley, P.J. and M. Vasak, *Possible role for metallothionein in protection against radiation-induced oxidative stress. Kinetics and mechanism of its reaction with superoxide and hydroxyl radicals*. Biochim Biophys Acta, 1985. **827**(1): p. 36-44.
11. Cai, L. and M.G. Cherian, *Zinc-metallothionein protects from DNA damage induced by radiation better than glutathione and copper- or cadmium-metallothioneins*. Toxicol Lett, 2003. **136**(3): p. 193-8.
12. Vasak, M. and D.W. Hasler, *Metallothioneins: new functional and structural insights*. Curr Opin Chem Biol, 2000. **4**(2): p. 177-83.
13. Iyer, L.M., A.M. Burroughs, and L. Aravind, *The ASCH superfamily: novel domains with a fold related to the PUA domain and a potential role in RNA metabolism*. Bioinformatics, 2006. **22**(3): p. 257-63.

14. Kim, H.J., et al., *Activating signal cointegrator 1, a novel transcription coactivator of nuclear receptors, and its cytosolic localization under conditions of serum deprivation*. Mol Cell Biol, 1999. **19**(9): p. 6323-32.
15. Otwinowski, Z. and W. Minor, *Processing of X-ray diffraction data collected in oscillation mode*. Methods Enzymol, 1997. **276**: p. 307-26.
16. Adams, P.D., et al., *PHENIX: a comprehensive Python-based system for macromolecular structure solution*. Acta Crystallogr D Biol Crystallogr, 2010. **66**(Pt 2): p. 213-21.
17. Emsley, P., et al., *Features and development of Coot*. Acta Crystallogr D Biol Crystallogr, 2010. **66**(Pt 4): p. 486-501.
18. Murshudov, G.N., A.A. Vagin, and E.J. Dodson, *Refinement of macromolecular structures by the maximum-likelihood method*. Acta Crystallogr D Biol Crystallogr, 1997. **53**(Pt 3): p. 240-55.

국문 초록

Endothelial-overexpressed lipopolysaccharide-associated factor 1 (EOLA1) 은 lipopolysaccharide의 활성화에 의해 내피 세포에서 발현된 novel gene이다. 이전 연구결과에 의하면, LPS가 처리된 human umbilical vein endothelial cells (HUVEC)에서 EOLA1의 억제제는 인터루킨-6 (IL6)와 apoptosis에 영향을 준다. Sequence 분석 결과, EOLA1은 pseudouridine synthase and archaeosine transglycosylase (PUA) 도메인의 독특한 β -배럴 fold와 비슷한 구조를 가진 activating signal cointegrator-1 homology (ASCH) 도메인을 가지고 있음을 알 수 있었다. PUA 도메인은 ancient RNA 결합 도메인이므로, ASCH와 PUA 도메인은 같은 RNA 결합 precursor인 것으로 보인다. 본 연구에서는 EOLA1의 구조를 1.7 Å으로 규명했고 selenomethionine derivative 결정을 통한 single wavelength anomalous dispersion (SAD)을 사용하여 phasing 문제를 해결했다. EOLA1은 5개의 α -helix (α A- α E)와 6개의 β -strands (β 1- β 6)으로 구성되었다. EOLA1의 결정 구조 분석 결과 ASC-1과 유사한 β -배럴 fold를 확인할 수 있었다. 더 나아가 gel mobility shift assay를 통해

EOLA1이 RNA와 결합을 할 수 있음을 보였다. 이러한 결과를 종합해 볼 때 본 연구자는 EOLA1이 RNA 결합 도메인이며 transcription 또는 HUVEC 염증 예방을 조절할 것이라고 제시한다.

2014-22967